ISSN 1063-7761, Journal of Experimental and Theoretical Physics, 2019, Vol. 129, No. 3, pp. 413–420. © Pleiades Publishing, Inc., 2019.
Russian Text © The Author(s), 2019, published in Zhurnal Eksperimental'noi i Teoreticheskoi Fiziki, 2019, Vol. 156, No. 3, pp. 493–501.

ORDER, DISORDER, AND PHASE TRANSITION IN CONDENSED SYSTEM

Effect of Impurities on the Oxygen Adsorption Properties on the NiTi(110) Surface

A. V. Bakulin[a,*] and S. E. Kulkova[b]

[a] *Institute of Strength Physics and Materials Science, Siberian Branch, Russian Academy of Sciences, Tomsk, 634055 Russia*
[b] *National Research Tomsk State University, Tomsk, 634050 Russia*
** e-mail: bakulin@ispms.tsc.ru*

Received February 25, 2019; revised March 5, 2019; accepted March 5, 2019

Abstract—The effect of 3*d*–5*d* elements on the oxygen adsorption energy on the NiTi(110) surface has been studied by the projector augmented-waves method within density functional theory. It is shown that almost all elements, except for a few elements of the end of *d* periods, lead to an increase in the adsorption energy if they substitute for nickel. On the contrary, the substitutional impurities in the titanium sublattice lower this energy. Based on the analysis of the electronic characteristics of the surface with impurities, it has been found that an increase/decrease in the oxygen adsorption energy on NiTi(110) correlates with a change in the ionic contribution to the mechanism of oxygen bonding with the surface.

DOI: 10.1134/S1063776119070033

1. INTRODUCTION

It is known that NiTi-based intermetallic alloys have unique mechanical properties, including shape-memory effect and superplasticity. They are widely used in various branches of the modern industry as electrical switches, connecting elements, fuses, thermal sensors, temperature controllers, satellite antennas, etc. Pins, various clamps, dental and bone implants, wire from nitinol (the name derived from the addition of the elements of the alloy and the laboratory where it was first obtained) are widely used in medicine. The interaction between the material from which the implant is made and human tissues is the main problem in medical applications. The biocompatibility of NiTi is believed to be the result of the formation of a thin inert TiO_2 film on its surface, which prevents the release of nickel [1]. Based on the experimental studies of NiTi wires with oxide layers of different thickness and thermodynamic analysis, Tian et al. [2] concluded that the appearance of Ni on the alloy surface can be prevented if the surface is fully oxidized. It is known that the interaction of titanium with oxygen may lead to the formation of several titanium oxides on the NiTi surface (Ti_2O, TiO, Ti_2O_3, Ti_3O_5, TiO_2), depending on the surface treatment methods [1]. In particular, it was shown in [2] that surface segregation of nickel in a thin oxide layer with oxygen deficiency is mainly due to atoms, although in thick oxide layers, surface segregation is dominated by metal particles. Earlier [3], we studied oxygen adsorption on the NiTi(110) surface and the atomic structure of the alloy–oxide interface using ab initio calculations, which provided additional information on nickel segregation. In particular, it was shown that the formation of single Ni defects is preferable in TiO over those in TiO_2, which confirms the conclusion drawn in [2]. Moreover, the calculations showed a significant increase in the defect formation energy in TiO_2, which indicates an increase in the activation energy of nickel diffusion in oxide. The mechanisms of nickel diffusion in NiTi were considered in [4], and the conclusion was that the probability of nickel diffusion along its own sublattice increases significantly with increasing temperature, although the six-jump mechanism along the [001] direction is preferable at low temperatures.

Improving the biocompatibility and corrosion resistance of NiTi is an important task of modern materials science. The latter can be achieved by modification of the alloy surface, since only it or several surface layers are in contact with human tissues. To modify the surface, magnetron sputtering and ion implantation of biotolerant chemical elements are used, which can form thin coatings on the surface of NiTi. Note that NiTi doping is also used to control the martensitic transformation, which is associated with the shape-memory effect [5]. At the same time, the segregation of impurities can significantly affect the adsorption of oxygen on the alloy surface, as well as the stability and strength of the TiO_2/NiTi interface. The effect of impurities on oxygen adsorption on the NiTi surface and on the adhesive properties of the interfaces of the alloy with oxides and metals has been poorly studied by theoretical methods. Therefore, the purpose of this work is a comparative study of the

effect of 3*d*–5*d* elements on oxygen adsorption on the stoichiometric NiTi(110) surface.

2. CALCULATION PROCEDURE

The atomic and electronic structure of the stoichiometric NiTi(110) surface with impurities in the surface layer and adsorbed oxygen was calculated using the projector augmented-waves (PAW) method in a plane wave basis [6, 7] using a VASP code [8, 9], with the generalized gradient approximation of the exchange-correlation functional in the GGA–PBE form [10]. The NiTi(110) surface was modeled by thin films separated by a vacuum gap of at least 15 Å. There were eleven atomic layers in the film, and the atoms of the three inner layers were fixed at the bulk positions, and the atoms of other layers of the film could relax in three directions. The relaxation of the atomic surface structure was carried out until forces at the atoms of about 0.01 eV/Å were attained. The energy cut-off of plane waves from the basis set was equal to 600 eV. The integration over the Brillouin zone in calculations of the electronic structure of the NiTi(110)-(2 × 2) surface was carried out using a *k*-points grid of 5 × 5 × 1 obtained by the Monkhorst–Pack scheme [11]. Note that the calculated equilibrium lattice parameter of *B*2-NiTi, equal to $a = 3.010$ Å, is in good agreement with an experimental value of 3.015 Å [12].

The oxygen adsorption energy was calculated by the formula:

$$E_{ads} = -1/2[E_{O/NiTiX} - E_{NiTiX} - E_{O_2}], \qquad (1)$$

where $E_{O/NiTiX}$ and E_{NiTiX} are total energies of the surface with oxygen and impurity (X) atoms in the surface layer and without oxygen, and E_{O_2} is the total energy of oxygen molecule. The factor 1/2 corresponds to oxygen adsorption on two alloy surfaces. For details on the calculations of oxygen adsorption on the undoped surface, see [3].

3. RESULTS AND DISCUSSION

We would like to say a few words about the results of calculation of the oxygen adsorption energy on the undoped NiTi(110) surface first of all. As was shown in our earlier work [3], the preferred position for oxygen adsorption on the NiTi(110) surface is the so-called three-fold coordinated *F*1 position above the triangle formed by two titanium and one nickel atoms (Fig. 1). An oxygen atom initially placed in the bridge position between the titanium and nickel atoms shifts during relaxation to this position. Note that the conclusion about the preference of this position differs from that obtained earlier by Nolan and Tofail [13]. In that work, the bridge Ti–Ni position is preferred, since the oxygen atom is only slightly shifted from it (Fig. 4b in [13]). Interestingly, the adsorption energy in the bridge position between nickel atoms (4.30 eV) obtained in [13] is only 0.07 eV lower in absolute value than in the preferred position. The adsorption energy in the *F*1 position is significantly higher (by 1.10 eV) than the highest energy obtained in [13]. Moreover, the oxygen adsorption energy in the bridge position between two titanium atoms is only 0.28 eV lower than in the *F*1 position. Note that this position was not considered in [13]. In general, the difference in the values of E_{ads} for other positions that were studied in both papers may be related both to the surface model used in the works and to the estimate of the total energy of an oxygen molecule. It is known that the binding energy in an oxygen molecule in the spin-polarized calculation differs from the experiment by approximately 1 eV. Moreover, the oxygen adsorption energy slightly increases with decreasing oxygen concentration on the surface. Thus, we found that oxygen on the NiTi(110) surface prefers to be adsorbed in positions enriched with titanium, that is consistent with the conclusion made for the TiAl alloy [14], as well as with experimental data [15]. Since oxygen prefers to form an ionic bond with metal surfaces, it occupies positions that allow one to obtain the necessary electrons to fill its *p* shell. As follows from these calculations, it is easier for oxygen to get these electrons from titanium than from nickel, since the *d* shell of the last element is almost completely occupied. According to the estimates of charge transfer by the Bader method [16], during the adsorption of oxygen in the *F*1 position, titanium loses 1.20*e*, and nickel, on the contrary, receives a charge of 0.51*e*. Slightly smaller values, 1.05*e* and 0.48*e*, were obtained by the DDEC6 method [17, 18]. As a result of the formation of titanium oxides on the NiTi(110) surface, the subsurface region is depleted in titanium, which causes the appearance of a nickel-rich layer, as shown in [2, 3]. In what follows, the influence of impurities is considered only in the preferred *F*1 position, and it is assumed that the impurity atom can be located on both the titanium and nickel sublattices, as shown in Fig. 1.

Figure 2 shows the results of calculations of the oxygen adsorption energy on the NiTi(110) surface, when the 3*d*–5*d* elements are in the surface layer near the *F*1 position and substitute for one of the two titanium atoms or a nickel atom. It is seen in Fig. 2 that the oxygen adsorption energy decreases for all impurities if they replace titanium, and, on the contrary, almost all 3*d* impurities except copper on the nickel sublattice lead to an increase in the oxygen adsorption energy. The tendencies in E_{ads} change due to the presence of 4*d* and 5*d* impurities on the nickel sublattice are similar: impurities of the beginning of periods up to the Group 7 elements with five *d* electrons on the outer shell increase the adsorption energy, but, with increasing number of valence electrons of the impurity atom, a decrease in the adsorption energy is observed. This decrease is less pronounced for the *d* elements of the end of periods, such as Cu, Ag, and Au. This behavior is due to the size effect, since oxygen shifts more strongly from Ag and Au than from other ele-

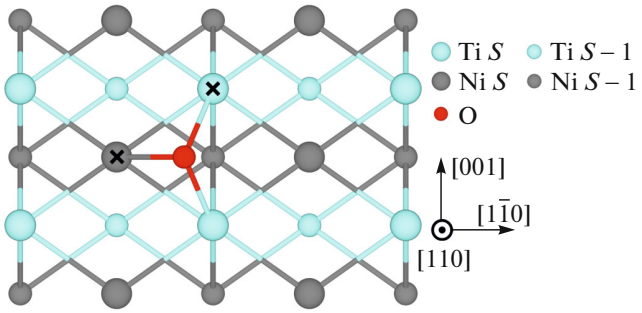

Fig. 1. (Color online) Atomic structure of the NiTi(110) surface with oxygen adsorbed in the most preferred $F1$-position. The positions of substitutional impurity atom on both sublattices are shown by crosses.

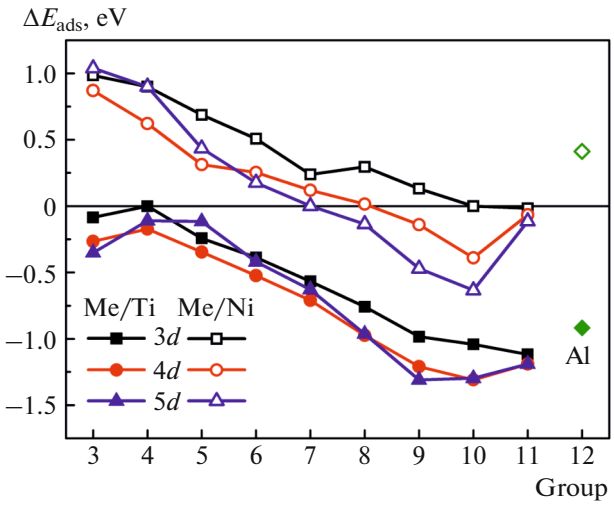

Fig. 2. (Color online) Change in the oxygen adsorption energy on the NiTi(110) surface depending on the number of d electrons on the outer shell of an impurity that substitutes for titanium or nickel atoms near the adsorption position.

ments, and in the latter case, is in the $F1$ position in the adjacent triangle as on an undoped surface. It should be noted that impurities of d elements of the beginning of periods prefer to occupy the titanium sublattice in the bulk NiTi alloy, as in TiAl [19], but already for Group 5 elements, this preference is less pronounced and may depend on the impurity concentration. As follows from our consideration in [20], other elements prefer to occupy the Ni sublattice.

In order to explain the trends in the binding energy of oxygen with the doped NiTi(110) surface, it is necessary to analyze changes in the density of states (DOS) of surface atoms. Figures 3a–3c show the corresponding DOS of atoms of the surface (S) and subsurface ($S-1$) layers when the impurities Nb, Rh, and Al are on the Ni sublattice, as shown in Fig. 1. Note that, for comparison, along with impurities of d metals, we considered Al, which, like Ti, has a high affinity for oxygen. As seen in Fig. 3a, the narrow valence oxygen 2p band lies below the bottom of the valence bands of the surface Ti and Nb atoms at energies from −6 to −4 eV. Since the oxygen 2s band is much lower, at energies of −19 eV, it is not shown in this figure. It is known that the interaction of oxygen with metals induces small peaks split from the bottom of their valence band. Thus, a small peak of the Ti split states is located at energies from −5.5 to −4.5 eV, where the oxygen 2p band is located. Since Nb has one more electron than Ti, its valence band shifts from the Fermi level (E_F) toward negative energies, while the split Nb peak is also located at practically the same energies as the Ti peak. Recall that the appearance of low-lying states and the formation of a pseudo-gap between them and the valence band is indicative of a change in chemical bond from metallic to ionic–covalent due to the initial stage of surface oxidation. As can be seen in Fig. 3a, the niobium valence band has a pronounced double-peak structure, with the bonding states making the main contribution to the DOS Nb peak at −0.4 eV, while the peak at about 3.2 eV is due to antibonding states. Since there is only a small density of states of Ti and Nb up to the Fermi level, the hybridization contribution to the binding energy of oxygen with the surface is small, and at energies from −4.0 eV up to the Fermi level, only a small density of oxygen states is observed. We note that the substituted nickel atom, whose density is shown by gray shading, on the contrary, has a broad peak in this energy range, centered at −2.0 eV. The proximity of the centers of gravity of the nickel and oxygen bands indicates that the hybridization energy is high [21, 22], but not all of the Ni states can be involved in the interaction, but only unpaired d electrons. As a result, the hybridization contributions of O–Ni and O–Ti to the binding energy of oxygen with an undoped surface are almost the same, as indicated by the calculation of overlap population on bonds (0.47e for O–Ti and 0.48e for O–Ni). At the same time, the ionicity of the O–Ti bond is much higher than that of O–Ni. This is clearly seen in Fig. 4a, which shows the distribution of the charge densities difference for an undoped surface. Recall that the electronegativities (χ) of titanium and nickel atoms are 1.54 and 1.91, respectively. It can be seen in Fig. 4b that the region of charge accumulation around oxygen is more strongly spread in the direction of Nb (χ is 0.31 lower than that of Ni) compared with the corresponding region in the direction of Ni on an undoped surface. This allows us to conclude that the ionicity of the O–Nb bond is also higher than that of O–Ni. Note that the O–Nb bond length (2.14 Å) is longer than the O–Ti bond length (1.93 Å), although the difference in the covalent radii of the two elements is only 0.02 Å. This indicates a stronger interaction of titanium with oxygen. As the calculation of charge transfer according to two schemes (Bader and DDEC6) showed, oxygen gets a 0.1e greater charge in the presence of niobium on the nickel sublattice. Note

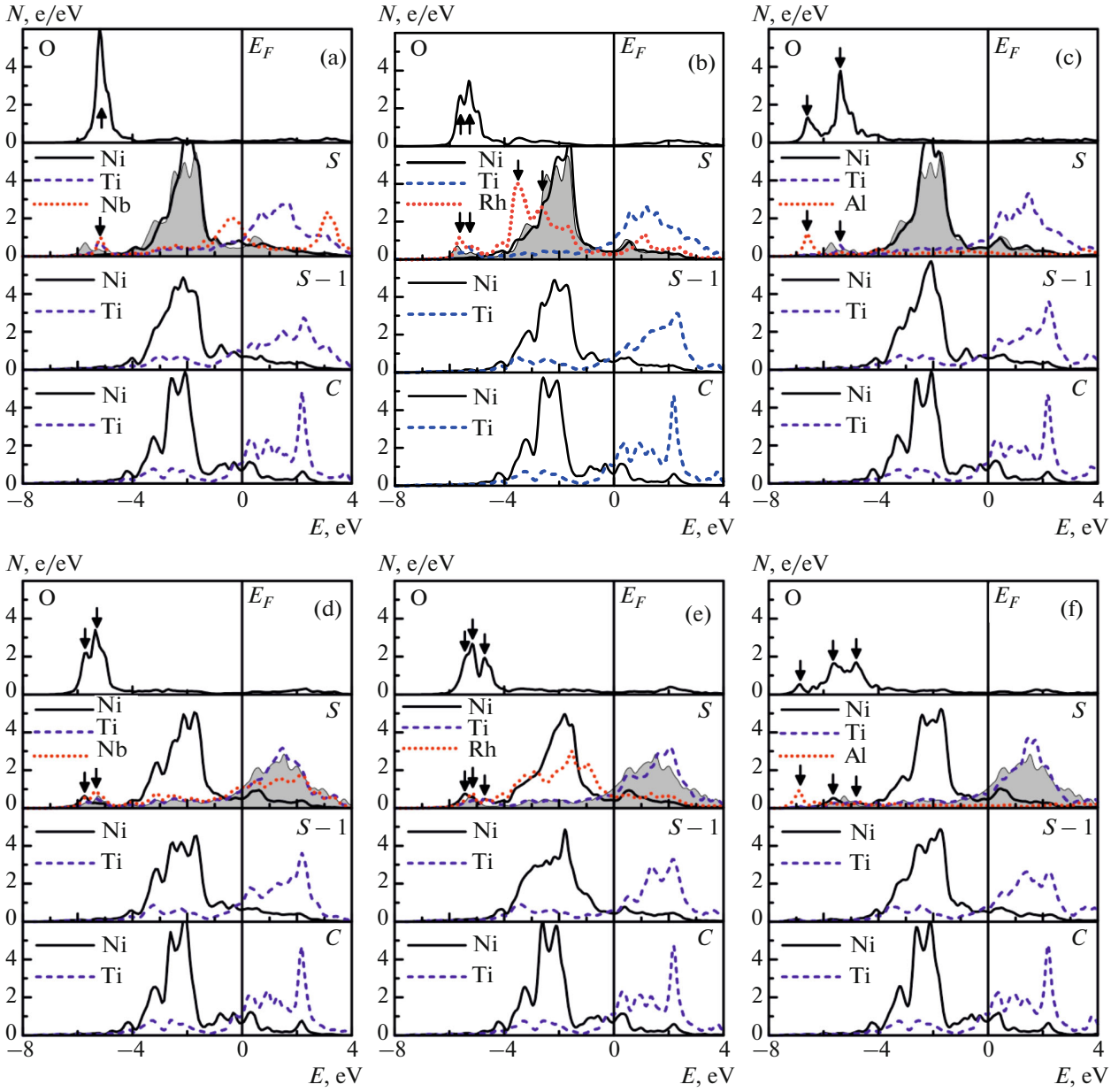

Fig. 3. (Color online) Local DOS of surface and subsurface atoms during oxygen adsorption on the NiTi (110)-(2 × 2) surface with impurities: Nb, Rh, and Al on the Ni sublattice (a–c); Nb, Rh, and Al on the Ti sublattice (d–f). Symbols *S*, *S* – 1, and *C* denote surface, subsurface, and bulk layers.

that other nickel atoms of both the surface and subsurface layers are also involved in interaction with oxygen, but this interaction is indirect, through hybridization with orbitals of surface titanium or niobium atoms. The interatomic distance between oxygen and the nearest surface nickel atoms is 3.13–3.68 Å, which is greater than the sum of their ionic radii and excludes direct interaction with oxygen. Figure 3a shows that the DOS of the surface nickel atom closest to oxygen on the doped surface differs only slightly from that of Ni on the undoped surface. In general, when niobium substitutes for nickel, the chemical bond of oxygen with NiTi(110) becomes stronger compared to undoped surface, because it interacts with three atoms with practically unoccupied *d*-shell, which provides an enhancement of the ionic contribution in the bonding mechanism (Fig. 4b) and an increase in the oxygen adsorption energy (Fig. 2).

If Rh is located on the Ni sublattice (Fig. 3b), then a more pronounced shift of the center of gravity of the occupied part of its valence band from the Fermi level is observed than in the case of Nb. Moreover, the main rhodium DOS peak is shifted toward negative energies by 1.7 eV relative to the of nickel DOS peak. This

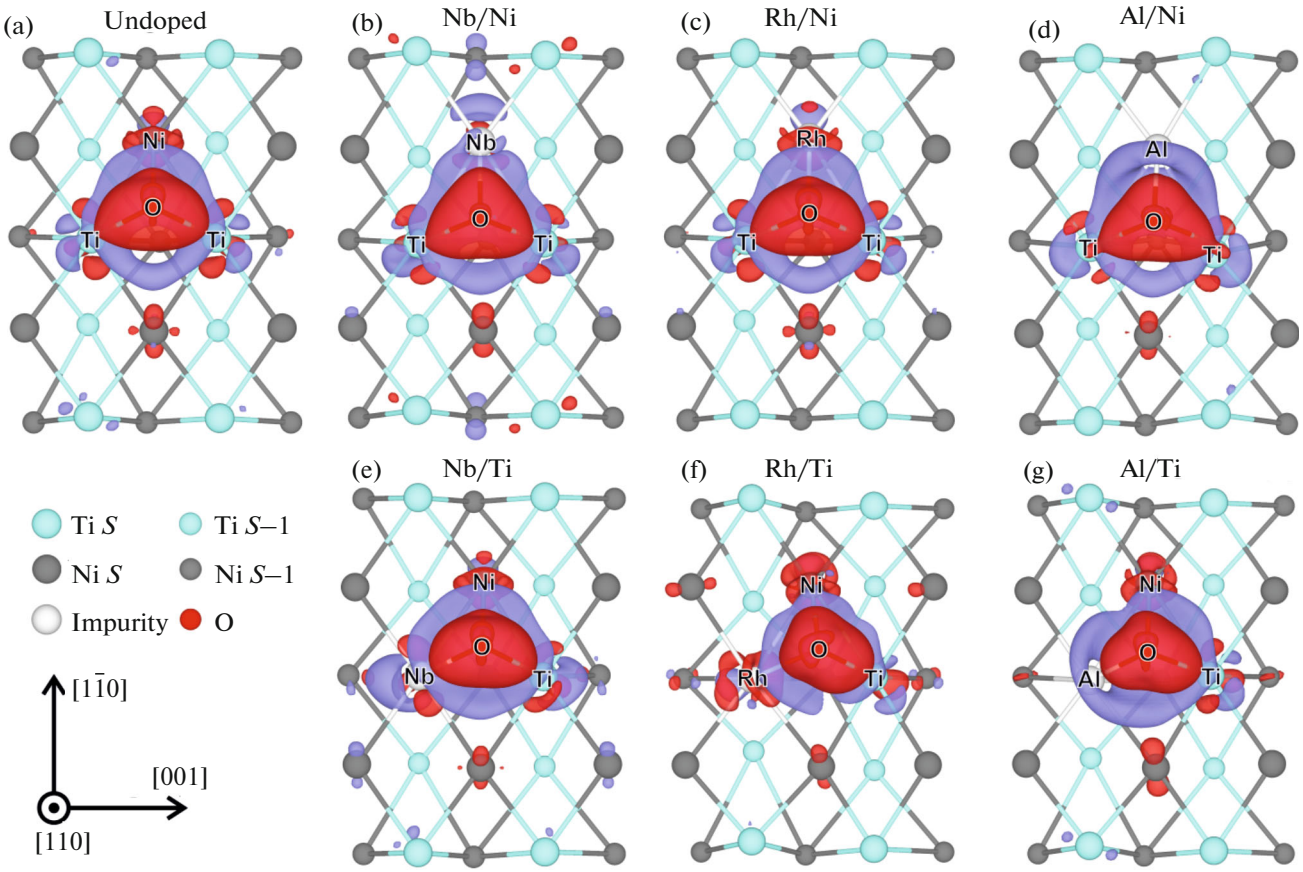

Fig. 4. (Color online) Distribution of the charge density difference ($\Delta\rho = \rho_O + \rho_{TiNiX} - \rho_{O/TiNiX}$) for the undoped surface (a) and the surface with impurities on Ni (b–d) and Ti sublattices (e–g). The regions of charge accumulation and depletion are shown in red and blue. The isosurfaces of charge density difference correspond to a charge of 0.025 e/Å^3.

should lead to increased hybridization of the *s*, *d* orbitals of Rh and the 2*p* states of O, especially since Rh has a greater number of unpaired electrons. It can be seen that in the energy range from –4.0 to –1.0 eV, the oxygen states become more pronounced and there are peaks of DOS at the same energies as on Rh DOS. The split peak of rhodium DOS is also shifted more strongly towards negative energies than the peak of titanium DOS, which leads to splitting of the main peak of oxygen DOS at an energy of –5.4 eV. In general, the fine structure of local Rh and O DOS correlates well. However, a detailed analysis of the crystal orbital Hamilton population (COHP) [23, 24] shows that states in the energy range from –4.0 to –1.0 eV are antibonding ones, as can be seen in Fig. 5, and do not contribute to the chemical bond of oxygen with rhodium. Note also that the overlap population on the O–Rh bond decreases by 7.7% compared with this characteristic on the O–Ni bond in case of undoped surface. The charge transfer to oxygen from the surface doped with rhodium ($\chi = 2.28$) or elements located to the right of it in the periodic table decreases slightly (Fig. 4c). Both factors determine a decrease in the oxygen adsorption energy in this case.

Finally, let us consider a situation when nickel is replaced by aluminum, which, like titanium, has a chemical affinity for oxygen. It is seen in Fig. 3c that the appearance of Al in the surface layer leads to the formation of a strong O–Al bond. It is known that delocalized *s*, *p* orbitals of Al are more easily involved in interaction with 2*p* states of oxygen than localized *d* states of Ti. This is confirmed by the appearance of split-off low-lying states of Al, the peak of which is lower in energy (–6.6 eV) than the peak of Ti (–5.3 eV). The corresponding peaks are shown by arrows in Fig. 3c. As a result of interaction with metals, the 2*p* band of O splits and becomes doubled with peaks at energies mentioned above. Note that the O–Al bond length is approximately 0.1 Å shorter than O–Ti (1.87 Å). Although the overlap population on the O–Al bonds increases by 34.2% compared with the overlap population on the O–Ti bonds, the contribution to the chemical bond due to the hybridization of the O 2*p* states with Al *s*, *p* orbitals is less than with Ti *s*, *d* orbitals. As shown by the analysis of charge transfer obtained by the Bader method, a charge of about 1.3*e* comes to oxygen in the presence of aluminum. It should be noted that charge transfer from tita-

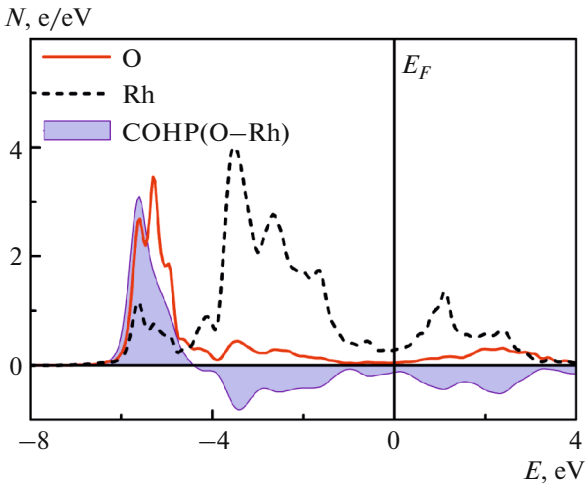

Fig. 5. (Color online) The densities of states of oxygen atoms and rhodium (on Ni sublattice) and COHP for the O–Rh bond shown by shading.

nium is weakly dependent on impurities. Thus, the enhancement of the ionic contribution (Fig. 4d) is partially compensated by a decrease in the hybridization contribution. The adsorption energy increases as in the case of niobium.

In the case of Nb on the Ti sublattice (Fig. 3d), the oxygen DOS decreases and slightly splits, which is caused by a shift of the Ni peak by about 0.3 eV relative to the split-off peak, to which Ti and Nb make the main contribution (shown by arrows in Fig. 3d). The number of occupied Nb states decreases (the peak below the Fermi level, which was noted above in Fig. 3a, is less pronounced and shifted toward positive energies), and the split-off Nb peak is shifted by 0.2 eV from the Fermi level compared to the case when it is located on the Ni-sublattice. The O–Nb bond length is 1.98 Å, which is significantly shorter than in the previous case. This indicates that the O–Nb interaction is increasing. It can be seen in Fig. 4e that the region of charge accumulation around oxygen only slightly differs from that for an undoped surface. At the same time, the enhancement of the Nb bond with both Ti and Ni leads to a smaller (approximately by 10.3%) charge transfer to oxygen. In general, a decrease in the oxygen adsorption energy is due to a decrease in the ionic contribution to the chemical bond.

In the case of Rh on the Ti sublattice (Fig. 3e), its states, as noted above, are practically at the same energies as the Ni states. The latter makes them compete for interaction with oxygen. It can be seen that the number of oxygen states in the energy range where Rh and Ni valence bands are located, increases, which should indicate an increase in the hybridization contribution to the binding energy; however, according to the COHP analysis, states above –4.0 eV are antibonding ones. At the same time, charge transfer to oxygen decreases by 0.10–0.15e, depending on the estimation method. As can be seen in Fig. 4f, the charge accumulation region spreads more towards Ti. The analysis of structural parameters shows that the impurity atom shifts towards the bulk, which leads to an increase in the O–Rh bond length (2.21 Å), which is 0.32–0.36 Å larger than O–Ni or O–Ti. Note that the distance from oxygen to the surface also increases with the filling of the d shell of impurities. Thus, regardless of the sublattice occupied, Rh lowers the oxygen adsorption energy.

If Ti is replaced by Al, then the DOS of oxygen decreases even more greatly and becomes more diffuse, and an almost split peak appears at –6.8 eV, due to its interaction with aluminum. It can be seen in Fig. 3f, that low-lying Al states spread to –7.6 eV. A change in the DOS of nickel is not that great compared with the corresponding curve on a undoped surface, which indicates a slight change in O–Ni hybridization. The ionic contribution decreases to a lesser extent than in the case of Rh on the Ti sublattice, since Al loses almost as many electrons as Ti (~1.25e). Note that not all of the charge from these atoms comes to oxygen. The main reason for a significant decrease in the oxygen adsorption energy in this case is a decrease in the O–Al hybridization contribution, as noted above. Note also that the DOS atoms of the subsurface layers have not previously been discussed, since their change, as can be seen in Fig. 3, is less pronounced than for surface atoms.

To conclude, we note that the trends of changes in the local DOS of surface oxygen and metal atoms remain almost the same for isoelectronic impurities. An increase in the adsorption energy by impurities of the end of the 3d period (Fig. 2) is explained by the greater chemical activity of these elements. It is known that both iron and cobalt form oxides more easily than isoelectronic 4d–5d metals. The same should be noted with respect to the 5d elements of the beginning of the period, for which the calculations show a greater increase in the adsorption energy than for the 4d-elements of the beginning of the period.

It should be noted that the characteristic mentioned above, such as the overlap population, is often used to estimate the hybridization contribution to the chemical bond, although they may not be accurate enough. The hybridization and ionic contributions to the binding energy of oxygen with the NiTi(110) surface for the considered impurities are schematically shown in Fig. 6. The increase in the population of orbitals by 38.8% for the Ti–Nb bond and by 27.4% for the Ti–Rh bond, when the impurity replaces nickel, as compared to this characteristic for the Ti–Ni bond on an undoped surface reflects the fact that more electrons can be involved in interaction with oxygen. Indeed, in the case of niobium on the Ni sublattice, an increase in both the hybridization and ionic contributions is observed, which correlates well with an increase in the adsorption energy (Fig. 6). Although

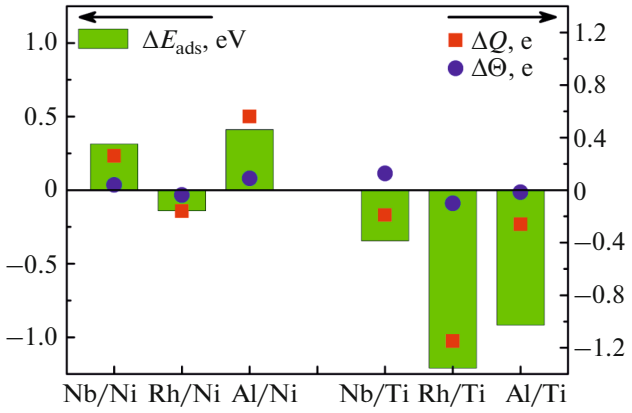

Fig. 6. (Color online) Changes in the oxygen adsorption energy on the NiTi(110) surface with doping of Nb, Rh, and Al, as well as changes in charge transfer to oxygen (ΔQ) and overlap population ($\Delta\Theta$) of orbitals of oxygen and impurity atoms.

the population of the orbitals of surface atoms in the case of Rh on the Ni sublattice increases on the surface without oxygen, the total overlap population on the O–Me bonds changes only slightly compared to the undoped surface. As shown in Fig. 6, the ionic contribution also decreases on the rhodium-doped surface, which correlates with a decrease in the adsorption energy. If *d*-metal impurities are on the Ti sublattice, then the population of the orbitals on the surface without oxygen also increases, as in the previous case, by 32.8% (Nb–Ni) and 11.1% (Rh–Ni). In this case, the hybridization contribution to the binding energy of oxygen with the surface increases substantially in the case of niobium and decreases slightly with doping of the surface by rhodium. However, as seen in Fig. 6, a decrease in the ion contribution is more significant for the considered impurities on the Ti sublattice. In the case of Al, on both sublattices, the trends in changes in the hybridization and ion contributions coincide.

We do not discuss results obtained for other impurities, since the trends remain valid for them too. Also, we would like to note that we did not take into account the mechanical contribution to the oxygen binding energy with the surface in the same way as it was done in our earlier work [25], since in this case, this contribution is an order of magnitude smaller than the chemical one. The effect of impurity on the oxygen binding energy with the surface is not discussed either if the impurity is in the subsurface layer, since its effect in this case is much less pronounced. It is believed that an increase in the oxygen adsorption energy may serve as an indication of an increase in the corrosion resistance of the alloy, but such a correlation needs a further study. It should be noted that, as was shown in our work [26], Zr, Nb, Mo, Hf, Ta, and W impurities are favorable for an increase in the formation energy of oxygen vacancies in TiO_2. The latter means decrease in alloy oxidation rate due to the suppression of oxygen diffusion through the oxide to the interface. It is known that a slower growth of the oxide film is favorable for the formation of a fully stabilized titanium oxide on the NiTi surface [27], with the possibility of stress relaxation at the alloy–oxide interface, which is important for the strength of these interfaces.

4. CONCLUSIONS

A comparative study of the effect of 3*d*–5*d* elements on the oxygen adsorption energy on the stoichiometric NiTi(110) surface by the projector augmented-waves method within density functional theory was carried out. It was found that 3*d*–5*d* impurities on the Ni sublattice, with the exception of a few elements of the end of *d* periods, lead to an increase in the adsorption energy, while it decreases for impurities on the Ti sublattice. It was shown that a decrease in the oxygen adsorption energy is less pronounced for impurities of elements of 3–5 Groups, if they occupy the most preferred Ti-sublattice. The impurities of the middle and end of the *d* periods prefer to substitute for Ni. The former slightly increase the adsorption energy, and the latter, on the contrary, decrease it, but to a much lesser extent than if they are on the Ti sublattice. For comparison, the effect on the adsorption energy of a *p* element, such as Al, which has a high affinity for oxygen, is considered. It was found that Al on the Ni sublattice increases, and on the Ti sublattice it lowers the oxygen adsorption energy. Using the example of Nb, Rh, and Al impurities, changes in the density of states of surface atoms, the charge density difference, charge transfer, overlap population on oxygen-metal bonds, and other properties were analyzed and compared with the corresponding characteristics for an undoped surface.

An increase in the number of states at energies from –4.0 to 0.0 eV found on the oxygen DOS does not always indicate a greater hybridization contribution to the bonding energy with the surface, since hybridized states at these energies can be antibonding as shown in the case of Rh. A change in the ionic contribution upon surface doping correlates well with the difference in the electronegativities of the impurity atom and the atom it substitutes for: in the case of Nb, which is more electronegative than Ti, this contribution decreases, but it increases in the case of substitution by Ni with a greater electronegativity. The same trend is observed for other impurities. A sharp increase in the adsorption energy in the case of Ag and Au impurities on the Ni sublattice compared to Pd and Pt is due to the size effect, namely, a greater shift of the oxygen atom away from the impurity and, as a consequence, a significant increase in its interaction with two titanium atoms. In general, it was shown that an increase/decrease in the oxygen adsorption energy on NiTi(110) correlates with a change in the ionic contribution to the mechanism of oxygen bonding to the surface.

FUNDING

This work was supported by project III.23.2.8 of the Institute of Strength Physics and Materials Science, Siberian Branch, Russian Academy of Sciences, and partly by the Russian Foundation for Basic Research (grant no. 18-03-00064_a) and Tomsk State University Competitiveness Improvement Program. Calculations were carried out using a supercomputer SKIF-Cyberia in Tomsk State University.

REFERENCES

1. S. A. Shabalovskaya, J. Anderegg, and J. Van Humbeeck, Acta Biomater. **4**, 447 (2008).
2. H. Tian, D. Schryvers, D. Liu, et al., Acta Biomater. **7**, 892 (2011).
3. S. E. Kulkova, A. V. Bakulin, Q. M. Hu, et al., Phys. B (Amsterdam, Neth.) **426**, 118 (2013).
4. A. V. Bakulin, T. I. Spiridonova, and S. E. Kulkova, Comput. Mater. Sci. **148**, 1 (2018).
5. V. G. Pushin, V. V. Kondrat'ev, and V. N. Khachin, *Transients and Martensitic Transformations* (UrO RAN, Yekaterinburg, 1998) [in Russian].
6. P. E. Blöchl, Phys. Rev. B **50**, 17953 (1994).
7. G. Kresse and D. Joubert, Phys. Rev. B **59**, 1758 (1999).
8. G. Kresse and J. Hafner, Phys. Rev. B **48**, 13115 (1993).
9. G. Kresse and J. Furthmüller, Comput. Mater. Sci. **6**, 15 (1996).
10. J. P. Perdew, K. Burke, and M. Ernzerhof, Phys. Rev. Lett. **77**, 3865 (1996).
11. H. J. Monkhorst and J. D. Pack, Phys. Rev. B **13**, 5188 (1976).
12. E. A. Brandes and G. B. Brook, *Smithells Metals Reference Book*, 7th ed. (Butterworth–Heinemen, London, 1992).
13. M. Nolan and S. A. M. Tofail, Biomaterials **31**, 3439 (2010).
14. A. V. Bakulin, S. E. Kulkova, Q. M. Hu, and R. Yang, J. Exp. Theor. Phys. **120**, 257 (2015).
15. M. Pohl, T. Glogowski, S. Kühn, et al., Mater. Sci. Eng. A **481–482**, 123 (2008).
16. W. Tang, E. Sanville, and G. Henkelman, J. Phys.: Condens. Matter **21**, 084204 (2009).
17. N. G. Limas and T. A. Manz, RSC Adv. **6**, 45727 (2016).
18. T. A. Manz and N. G. Limas, RSC Adv. **6**, 47771 (2016).
19. A. V. Bakulin and S. E. Kulkova, J. Exp. Theor. Phys. **127**, 1046 (2018).
20. S. E. Kulkova, A. V. Bakulin, Q. M. Hu, et al., Mater. Today: Proc. **2S**, 615 (2015).
21. B. Hammer and J. K. Nørskov, Surf. Sci. **343**, 211 (1995).
22. V. E. Egorushkin, S. E. Kul'kova, N. V. Mel'nikova, and A. N. Ponomarev, J. Exp. Theor. Phys. **101**, 350 (2005).
23. R. Dronskowski and P. E. Blöchl, J. Phys. Chem. **97**, 8617 (1993).
24. S. Maintz, V. L. Deringer, A. L. Tchougreeff, et al., J. Comput. Chem. **37**, 1030 (2016).
25. S. E. Kulkova, A. V. Bakulin, S. S. Kulkov, et al., Phys. Scr. **90**, 094010 (2015).
26. F. P. Ping, Q. M. Hu, A. V. Bakulin, et al., Intermet. **68**, 57 (2016).
27. G. S. Firstov, R. G. Vitchev, H. Kumar, et al., Biomaterials **23**, 4863 (2008).

Translated by A. Zeigarnik